CANCER

An antibody-drug conjugate directed to the ALK receptor demonstrates efficacy in preclinical models of neuroblastoma

Renata Sano[1], Kateryna Krytska[1], Colleen E. Larmour[1], Pichai Raman[2], Daniel Martinez[3], Gwenda F. Ligon[4], Jay S. Lillquist[4], Ulisse Cucchi[5], Paolo Orsini[5], Simona Rizzi[5], Bruce R. Pawel[3], Diego Alvarado[4], Yael P. Mossé[1,6]*

Enthusiasm for the use of antibody-drug conjugates (ADCs) in cancer therapy has risen over the past few years. The success of this therapeutic approach relies on the identification of cell surface antigens that are widely and selectively expressed on tumor cells. Studies have shown that native ALK protein is expressed on the surface of most neuroblastoma cells, providing an opportunity for development of immune-targeting strategies. Clinically relevant antibodies for this target have not yet been developed. Here, we describe the development of an ALK-ADC, CDX-0125-TEI, which selectively targets both wild-type and mutated ALK-expressing neuroblastomas. CDX-0125-TEI exhibited efficient antigen binding and internalization, and cytotoxicity at picomolar concentrations in cells with different expression of ALK on the cell surface. In vivo studies showed that CDX-0125-TEI is effective against ALK wild-type and mutant patient-derived xenograft models. These data demonstrate that ALK is a bona fide immunotherapeutic target and provide a rationale for clinical development of an ALK-ADC approach for neuroblastomas and other ALK-expressing childhood cancers such as rhabdomyosarcomas.

INTRODUCTION

Neuroblastoma is a pediatric cancer of the peripheral sympathetic nervous system that accounts for 12% of all childhood cancer mortality (*1*, *2*). Children with the high-risk form of the disease continue to have poor outcomes despite dose-intensive therapy. Recently, a chimeric monoclonal antibody (mAb) targeting the disialoganglioside GD2, given with cytokines for patients in first remission, showed improved outcomes in a phase 3 trial (*3*), leading to subsequent U.S. Food and Drug Administration (FDA) approval. This credentialing of immunotherapy for neuroblastoma, coupled with the recent successes of chimeric antigen receptor (CAR) T cell therapy in childhood acute lymphoblastic leukemia (*4*, *5*), has created unique translational opportunities to study immunotherapies for pediatric cancers. However, a major challenge remains in identifying cell surface molecules that meet the stringent criteria for optimal safety and therapeutic efficacy. Despite decades of research on GD2, the neuroblastoma cell surface proteome remains largely unexplored. Furthermore, although a mAb targeting GD2 (dinutuximab) has become the first FDA-approved therapy for children with high-risk neuroblastoma, it is a very toxic therapy, with pain and anaphylaxis as common causes for drug discontinuation, and relapse still occurring in at least half of patients.

A recent study has nominated glypican-2 (GPC2) as a candidate immunotherapeutic target in neuroblastoma, providing a foundation for further development of GPC2-directed immune-based therapies (*6*), but little is known about the neuroblastoma surfaceome. We and others have shown that germline gain-of-function mutations in the kinase domain of the anaplastic lymphoma kinase (ALK) oncogene, located in the plasma membrane, result in heritable susceptibility to develop neuroblastoma (*7*, *8*). *ALK* is also the most common somatically mutated gene in neuroblastoma (*8*–*11*), and small-molecule inhibitors of ALK kinase activity have been rapidly developed and translated to early-phase clinical trials (*12*–*16*). However, several of the common recurrent mutations result in de novo resistance to adenosine 5′-triphosphate (ATP)–competitive small molecular inhibitors, potentially limiting their utility in this disease (*9*, *10*). We have previously shown that native ALK protein is expressed on the surface of the majority of neuroblastoma cells with or without germline or somatic *ALK* mutations, but not on normal tissue, providing an opportunity for development of ALK-targeting antibodies bearing cytotoxic payloads (*17*). In addition, the recent discovery of the ALK ligand (*18*, *19*) may have an impact on ALK expression and activation in neuroblastoma.

Targeting ALK with an antibody-drug conjugate (ADC) is one such potential therapeutic strategy. ADCs are a rapidly growing class of anticancer drugs that combine the targeting properties of mAbs (*20*) with the antitumor effects of potent cytotoxic drugs (*21*). Currently, four ADCs have been approved for use in the United States and Europe: Adcetris (brentuximab vedotin) in 2011 for the treatment of refractory Hodgkin's lymphoma and anaplastic large cell lymphoma; Kadcyla (ado-trastuzumab emtansine) in 2013 for the treatment of HER2-overexpressing metastatic breast cancer: Besponsa (inotuzumab ozogamicin) in 2017, indicated for the treatment of CD22-related acute lymphoblastic leukemia; and a fourth ADC, Mylotarg (gemtuzumab ozogamicin), which has been recently reapproved for the treatment of CD33-positive acute myeloid leukemia (AML) patients (*22*).

We describe the identification of an antibody suitable for an ADC approach with consideration of target specificity, affinity, internalization into target-expressing cells, and cross-species reactivity. We present preclinical data on the activity of an ALK-directed ADC (CDX-0125-TEI) consisting of CDX-0125, an anti-ALK mAb, coupled to interchain

[1]Division of Oncology and Center for Childhood Cancer Research, Children's Hospital of Philadelphia, Philadelphia, PA 19104, USA. [2]Division of Oncology and Center for Biomedical Informatics (CBMi), Children's Hospital of Philadelphia, Philadelphia, PA 19104, USA. [3]Department of Pathology, Children's Hospital of Philadelphia and Department of Pediatrics, University of Pennsylvania School of Medicine, Philadelphia, PA 19104, USA. [4]Celldex Therapeutics Inc., New Haven, CT 06511, USA. [5]Nerviano Medical Sciences S.r.l., Nerviano (MI) 20014, Italy. [6]Department of Pediatrics, Perelman School of Medicine at the University of Pennsylvania, Philadelphia, PA 19104, USA.
*Corresponding author. Email: mosse@chop.edu

cysteine residues via a dipeptidic cleavable linker to a thienoindole (TEI) DNA minor groove alkylating agent (*23*). CDX-0125-TEI demonstrates antitumor activity in ALK-expressing models of human neuroblastoma, both in vitro and in vivo. Furthermore, antitumor activity was observed independent of *ALK* mutation status. The results presented here support further development of ALK-targeted ADCs with potential utility in ALK-expressing pediatric tumors.

RESULTS

ALK-specific mAbs were generated and characterized

We previously demonstrated that a tool ALK antibody, which is not available for clinical development, was effective at inducing antibody-dependent cellular cytotoxicity (ADCC) and immune cell–independent growth inhibition and cytotoxicity against a single ALK mutant neuroblastoma cell line (*17*). To further develop this concept, we generated a panel of 32 ALK-targeting mAbs by immunizing mice with a purified human ALK antigen encompassing the extracellular domain. Hybridoma-derived murine mAbs were evaluated for binding to ALK-expressing neuroblastoma cells, apparent affinity, domain binding, and activity in phosphorylation and proliferative assays. mAbs that demonstrated both strong binding to ALK-expressing NB-1 cells and modulation of ALK phosphorylation in these cells were converted to human immunoglobulin G1 (IgG1) heavy and light constant regions. Nine antibodies with low dissociation constant (K_d) and strong reactivity to ALK were prioritized (table S1) for further evaluation to assess their inhibitory properties as unconjugated antibodies.

We performed viability assays with increasing concentrations of each antibody against the NB-1 cell line, which harbors high-level *ALK* amplification and protein expression (*10*). Whereas crizotinib induced the expected concentration-dependent decrease in cell viability (*12*, *13*), we observed no evidence of cytotoxicity with the candidate ALK antibodies when compared to IgG-treated controls (fig. S1A). None of the candidate antibodies exhibited growth inhibitory properties when administered to an expanded panel of human neuroblastoma–derived cell lines harboring wild-type (NB-EBc1 and NB-1691) or mutated ALK (NB-1643, R1275Q; SH-SY5Y, NBS-D; and Kelly, F1174L). No cytotoxicity was observed compared to the IgG control upon treatment for different amounts of time (4 to 72 hours) or upon combination of antibodies with distinct epitope specificity. Furthermore, we did not observe enhanced cytotoxicity upon combining crizotinib with the varying candidate ALK antibodies in cells harboring de novo resistant *ALK* mutations (*17*).

From these, mAb CDX-0125 exhibited potent binding to ALK-expressing cells, rapid internalization, cross-species reactivity (mouse and human), and inhibited (rather than stimulated) basal ALK phosphorylation in NB-1 cells (fig. S1B), rendering it as an appropriate candidate for conjugation to a cytotoxic agent. We pursued in vitro analyses of ADCC using aCella-TOX, a coupled bioluminescent method that measures glyceraldehyde-3-phosphate dehydrogenase (GAPDH) release from target cells. Using GD2, which has been extensively studied as the primary target of antibody recognition in neuroblastoma (*24*, *25*), as a positive control, we found that CDX-0125 was not capable of exerting an ADCC effect when tested against the NB-1 cell line (fig. S1C). Although high concentrations of extracellular GAPDH were detected in samples treated with anti-GD2 ch14.18 at 25 μg/ml, samples incubated with the anti-ALK antibody CDX-0125, across a range of concentrations, showed no evidence of ADCC (fig. S1C). Together, these results demonstrated that none of these antibodies had meaningful antiproliferative activity, nor could they induce an immune-mediated antitumor response in neuroblastoma cell lines.

ALK is expressed on the surface of most neuroblastomas and not in normal tissues

We next exploited CDX-0125 for quantification of plasma membrane ALK expression using flow cytometry in a panel of human neuroblastoma–derived cell lines expressing either wild-type ALK (SK-N-AS, NB-1691, and NBL-S) or mutated or amplified ALK (NB-1643, SH-SY5Y, COG-N-453, SMS-SAN, Felix, and NB-1) using molecules of equivalent soluble fluorochrome (MESF) methodology (*26*). The data showed highly variable ALK expression across these models, with no correlation to underlying ALK mutation status (Fig. 1A).

In addition, we optimized an immunohistochemical (IHC) assay using a commercially available anti-ALK mAb to evaluate ALK expression on a panel of 32 patient-derived xenografts (PDXs) from high-risk human primary tumors in tissue microarrays (TMAs). Surface ALK expression was quantified by converting the staining intensity (range, 0 to 3) and the percentage of cells with expression to an H-score (range, 0 to 300). A total of 63% of cores (20 of 32) had a membrane staining H-score of 100 or greater, confirming high expression of ALK on the cell surface in the majority of neuroblastoma tumors (Fig. 1, B and C, and fig. S2A). We next explored ALK expression on the surface of cells from dissociated PDX tumors with both immunoblotting and flow cytometry using a phycoerythrin (PE)–conjugated ALK antibody. Immunoblotting (Fig. 1D) and semiquantitative analysis (Fig. 1E) of four mouse-depleted PDX homogenates showed differential ALK expression, consistent with the IHC H-scores. Upon quantitative analysis of MESF, we demonstrated a similar range of cell surface ALK expression (Fig. 1F). Last, we performed IHC with the same antibody on a comprehensive normal pediatric TMA ($n = 36$ pediatric normal tissues that cover all the major human organs) and showed absent staining in all cores (fig. S2B). Collectively, our data show that ALK is widely expressed on the cell surface of most neuroblastoma cell lines and PDX tumors, and its expression appears to be restricted to tumor tissue.

CDX-0125 is efficiently internalized after binding ALK

To determine if an ADC approach might be considered for immunotherapeutic targeting of ALK in neuroblastoma, we examined internalization kinetics after treating neuroblastoma cells with CDX-0125. We titrated CDX-0125 in the high ALK–expressing human NB-1 neuroblastoma and murine Neuro-2a cells and showed robust binding with an apparent dissociation constant of about 500 pM; conversely, CDX-0125 binding to the ALK-null cell line SK-N-AS was not observed (Fig. 2A). Here, we used two approaches: a qualitative immunofluorescence staining and a quantitative flow cytometric analysis. Internalization of Alexa 488–conjugated CDX-0125, after binding to NB-1 cells, was visualized by microscopy. At 4°C, CDX-0125–Alexa 488 showed distinct membrane localization (Fig. 2B, left). Conversely, after incubation at 37°C for 4 hours, membrane localization was markedly reduced and CDX-0125 appeared as punctuated intracellular aggregates throughout the cytosol (Fig. 2B, right). To corroborate these cell imaging data, we quantitatively assessed antibody internalization as a function of time in six cell lines with differential expression of cell surface ALK. Upon CDX-0125 antibody

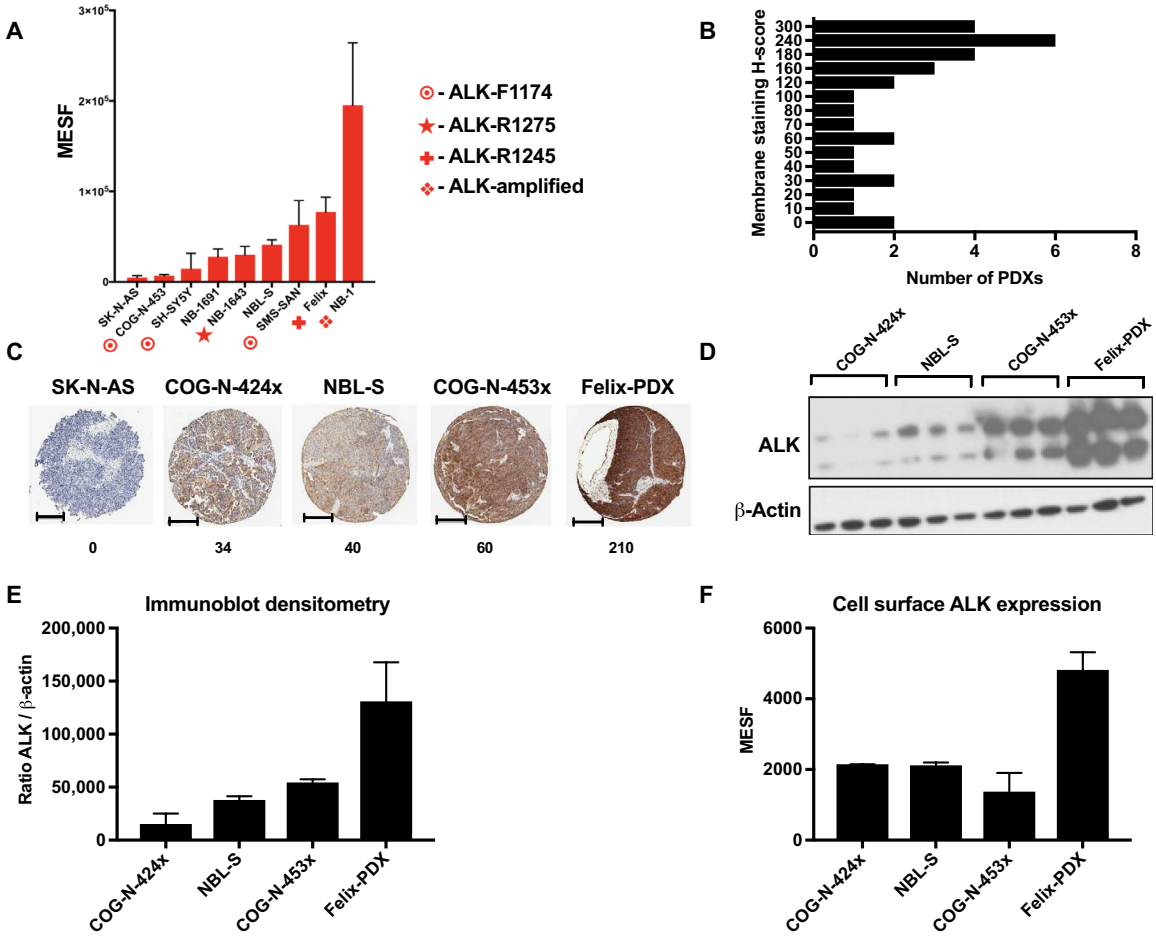

Fig. 1. ALK is widely expressed in neuroblastoma. (**A**) Cell surface ALK was quantified in a representative panel of nine neuroblastoma-derived cell lines expressing amplified (NB-1), wild-type (NB-1691 and NBL-S), or mutated ALK [SH-SY5Y, F1174L; COG-N-453, F1174L; NB-1643, R1275Q; SMS-SAN, F1174L; and Felix, F1245C (indicated with red symbols)]. Data are shown as means ± SD (n = 2 to 8). (**B**) ALK expression was determined by TMA analysis of 32 different neuroblastoma PDX models. Expression was quantified via determination of H-scores, which takes into consideration the staining intensity in conjunction with the percentage of cells staining positively. (**C**) Representative H-scores and staining patterns are shown in a subset of samples: SK-N-AS (null), COG-N-424x (moderate), NBL-S (moderate), COG-N-453x (moderate), and Felix-PDX (strong). Scale bars, 200 μm. (**D**) A fraction of mouse-depleted homogenates was subjected to immunoblotting analysis to determine ALK expression. β-Actin was used as a loading control. (**E**) ALK bands visualized in (D) were quantitated using densitometry analysis and expressed as the ratio of ALK signal over β-actin signal. Data are presented as means ± SD (n = 3). (**F**) Flow cytometry analysis was performed in mouse-depleted dissociated PDXs, and fluorescence was quantitated on the basis of MESF using standard beads. Data are presented as means ± SD (n = 2).

binding, cells were further incubated at 37°C at the indicated time points (Fig. 2C)—10 to 60 min—and subsequently stained with a fluorescent secondary antibody. Internalized CDX-0125 was indirectly calculated by subtracting the fluorescence units detected in 37°C-incubated cells from the fluorescence of cells in which only binding was allowed to occur at 4°C for 1 hour. The extent of CDX-0125 internalization in each cell line differed considerably and was proportional to the magnitude of cell surface ALK expression. For instance, cells harboring amplified ALK (NB-1) internalized high amounts of CDX-0125 over time compared to IMR-32 and SK-N-AS, both cell lines with low or null ALK expression.

An ALK ADC was developed by conjugation of CDX-0125 with DNA-alkylating agent NMS-P945

We explored two distinct classes of linker and toxin platforms to select the ADC with the highest potential for efficacy. In addition to potency, we considered several other properties of the cytotoxic payloads, including chemical structure and drug resistance mechanisms. CDX-0125-TEI was generated by the conjugation of purified CDX-0125 to the TEI derivative NMS-P945, a DNA minor groove alkylating agent bearing a peptidic cleavable drug linker and a self-immolative spacer (Fig. 2D), which, through lysosomal enzyme cleavage inside the tumor cells, allows the release of the free toxin NMS-P528. NMS-P945 is conjugated to CDX-0125 through partial reduction of interchain cysteine residues, yielding an average drug-antibody ratio (DAR) of 2.7, and >95% monomer content. We showed that conjugating CDX-0125 to this TEI DNA-alkylating agent resulted in much greater ALK-dependent cytotoxicity in neuroblastoma cells than conjugation with a tubulin-disrupting agent (fig. S3), a difference observed in two human neuroblastoma–derived cell lines (ALK wild-type IMR-32 and ALK mutant SK-N-SH), which supported further evaluation of the TEI as the payload for CDX-0125.

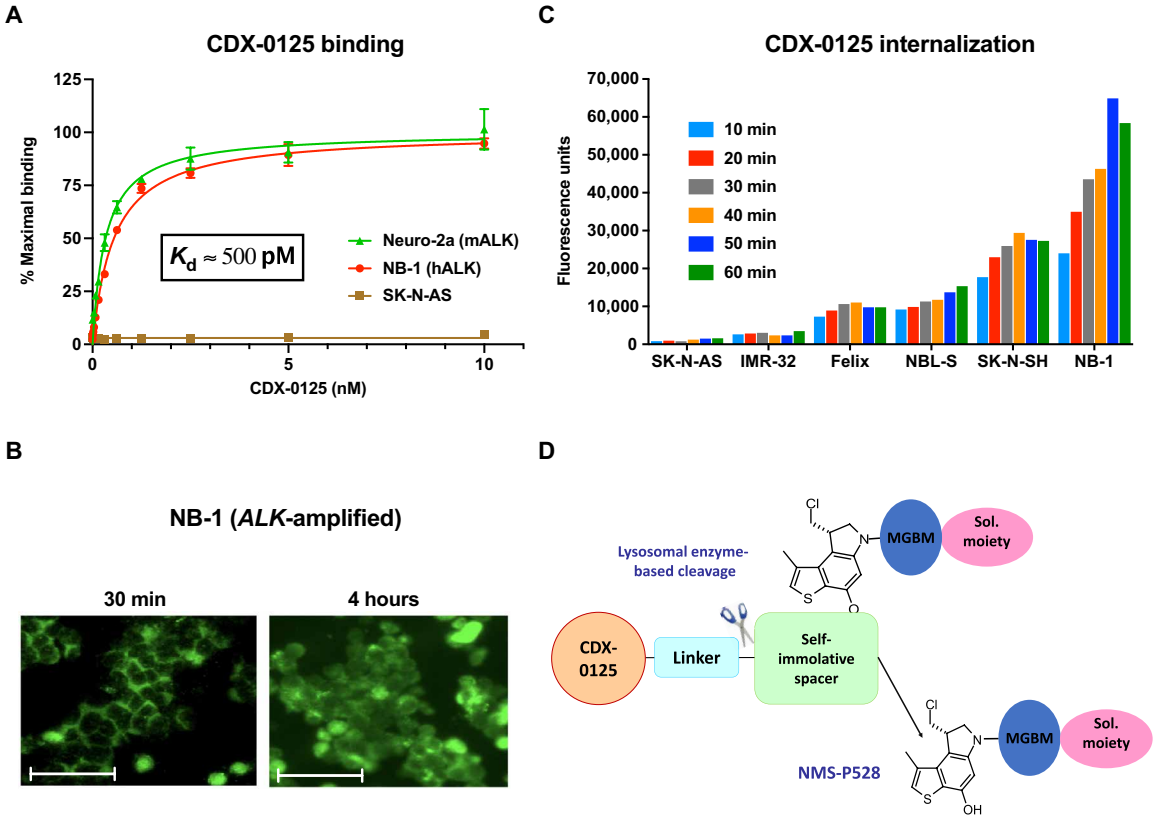

Fig. 2. CDX-0125-TEI efficiently binds to cell surface ALK and is internalized. (**A**) CDX-0125-TEI binds to both mouse (Neuro-2a) and human ALK (NB-1) with picomolar affinity and does not bind to SK-N-AS cells, an ALK-null line. Experiments were performed three independent times. Data are presented as means ± SEM (n = 3). (**B**) Representative images of immunofluorescence experiments showing localization of CDX-0125-TEI at the cell membrane (30 min at 4°C, left) and at the cytoplasm of NB-1 cells (4 hours at 37°C, right). Scale bars, 50 μm. (**C**) Quantitative internalization of CDX-0125 in NB-1, Felix, NBL-S, SK-N-SH, IMR-32, and SK-N-AS cells over a 60-min time course. Data are presented as mean values (n = 2 to 3). (**D**) Schematic illustration of the CDX-0125-TEI molecule. The TEI NMS-P528 bearing a minor groove binding moiety (MGBM) is released after peptidic cleavage by lysosomal proteases and spacer self-immolation, resulting in the removal of the protective moiety and release of the toxin.

CDX-0125-TEI demonstrates in vitro cytotoxicity against ALK-expressing cells

The cytotoxic activity of CDX-0125-TEI against a panel of four human neuroblastoma–derived cell lines expressing different forms and amounts of cell surface ALK was evaluated using cell viability assays. The toxin was potently cytotoxic across all four neuroblastoma cell lines regardless of ALK expression or mutation status (Fig. 3). CDX-0125-TEI yielded median inhibitory concentration (IC_{50}) values of 5.8 pM against NB-1 (ALK-amplified), 4.7 pM against IMR-32 (ALK wild type), 21.7 pM against SK-N-SH (ALK F1174L), and >1000 pM against SK-N-AS (ALK null). Despite the similar activity observed for the TEI-free toxin NMS-P528 in all tested cell lines, robust killing was seen for CDX-0125-TEI in all three ALK-expressing cell lines, but not in the SK-N-AS cell line, where ALK expression is not detectable. To further confirm on-target killing by CDX-0125-TEI, we used a nonbinding control human IgG1 conjugated to TEI and observed minimal cytotoxicity activity with this negative control, IgG1-TEI (Fig. 3). Collectively, these data demonstrate that CDX-0125-TEI mediates cytotoxicity in an antigen-dependent manner.

CDX-0125-TEI induces single-strand DNA damage and apoptosis

The payload in CDX-0125-TEI is a potent minor groove alkylating compound that covalently modifies DNA by generating inter- and intrastrand cross-links (*23*, *27*). We evaluated the ability of CDX-0125-TEI to induce single-strand DNA damage using an assay designed to quantify sensitivity of DNA to thermal denaturation in condensed chromatin of apoptotic cells (*28*). After 5 days of treatment with either CDX-0125-TEI or toxin alone (NMS-P528) at their respective IC_{50} concentrations, NBL-S, Felix, and NB-1 cells showed more than twofold increase in F7-26 staining over control IgG (fig. S4). Conversely, the ALK-null SK-N-AS cells showed sensitivity restricted to NMS-P528 alone and SN-38, the active drug released by irinotecan. Furthermore, annexin V staining showed induction of apoptosis in a panel of neuroblastoma cells treated with either CDX-0125-TEI or NMS-P528 alone (Fig. 4A), as well as induction of the apoptosis marker cleaved caspase-3 demonstrated by immunoblotting in the relatively high ALK–expressing NBL-S cells (Fig. 4B) and, to a lesser extent, in low ALK–expressing COG-N-453 cells (Fig. 4C). These data show on-target activity of CDX-0125-TEI, with apoptosis observed even in cells with low receptor density.

CDX-0125-TEI is effective against ALK wild-type and mutant PDX models

Efficacy of CDX-0125-TEI was initially evaluated in two PDX models with varying ALK expression and mutation status, Felix-PDX (ALK F1245C) and COG-N-453x (ALK F1174L). Tumor-bearing animals were randomized to treatment by intraperitoneal injections with

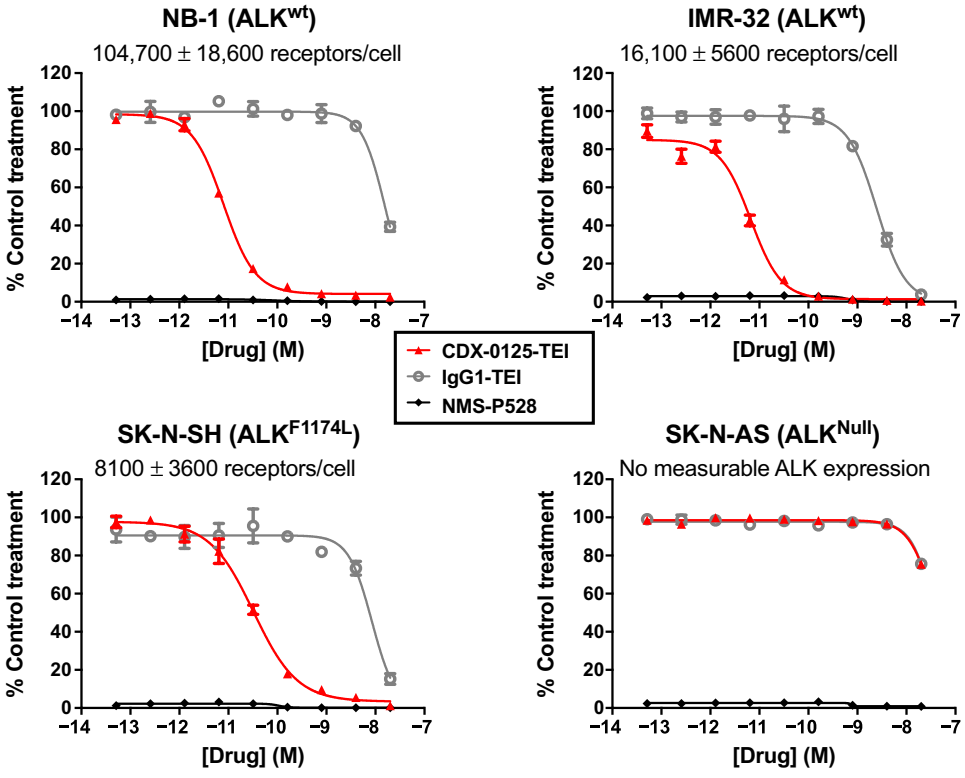

Fig. 3. CDX-0125-TEI is cytotoxic to ALK-expressing neuroblastoma cells in vitro. Neuroblastoma cells expressing wild-type ALK (NB-1 and IMR-32) and mutated ALK (SK-N-SH) or with no detectable ALK expression (SK-N-AS) were treated with increasing doses of CDX-0125-TEI, a control IgG1 antibody conjugated with TEI (IgG1-TEI), or the free payload (NMS-P528). Titration of CDX-0125-TEI induced cytotoxic activity in all ALK-expressing models, with IC_{50} values in the picomolar range and independent of ALK mutation status or number of cell surface ALK receptors. By contrast, no measurable IC_{50} value could be derived in the ALK-negative cell line SK-N-AS. Free NMS-P528 elicited complete cell killing at sub-picomolar concentrations in all cell lines tested. Quoted IC_{50} and ALK expression values reflect calculated means and SEM ($n = 3$) from at least three independent experiments.

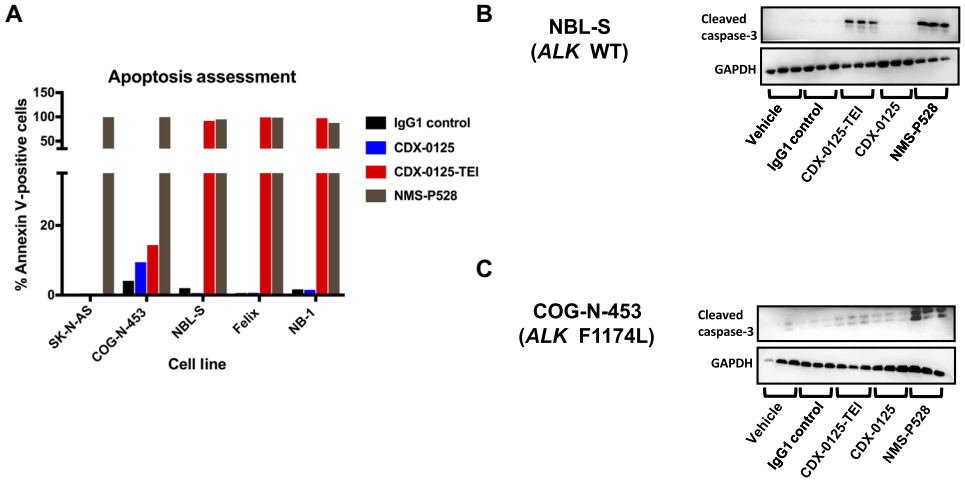

Fig. 4. CDX-0125-TEI induces apoptosis. (**A**) Apoptosis was quantified by annexin V–FITC (fluorescein isothiocyanate) and analyzed by FACS (fluorescence-activated cell sorting) in neuroblastoma cells (SK-N-AS, COG-N-453, NBL-S, Felix, and NB-1) treated with CDX-0125, CDX-0125-TEI, NMS-P528, or IgG1 control at their predetermined IC_{50} values. Values from a representative experiment are shown. Experiments were performed three independent times. (**B**) NBL-S and (**C**) COG-N-453 were subjected to immunoblot analysis and probed for the apoptosis marker cleaved caspase-3 and GAPDH as a loading control. Each bracket represents three independent samples. WT, wild type.

IgG, unconjugated CDX-0125, or CDX-0125-TEI once a week for two consecutive weeks at a range of doses: 1, 3, and 10 mg/kg (Fig. 5). Although CDX-0125-TEI binds potently to mouse ALK and human ALK, CDX-0125-TEI was well tolerated with no observed overt toxicities. Significant tumor growth delay was achieved in Felix-PDX after two injections of CDX-0125-TEI (Fig. 5A), and this was dose dependent (Fig. 5A and table S2; $P < 0.0001$). Tumor growth delay was initially achieved, but all tumors progressed starting at about 2 weeks from the second injection (Fig. 5A). CDX-0125-TEI was less effective against COG-N-453x (Fig. 5B) despite a survival benefit (table S2). A dose-dependent induction of cleaved caspase-3 was seen in all tested models (fig. S5). Although we observed down-regulation of phosphorylated ALK in the tumors treated with doses of 1 and 3 mg/kg, we believe that this effect was transient and not biologically relevant, given that tumors were harvested only 4 hours after the second injection, a time point at which CDX-0125-TEI may not have been fully cleared in vivo.

Because the majority of primary neuroblastoma tumors express native ALK, we evaluated the efficacy of CDX-0125-TEI in two ALK-expressing/ALK wild-type models, COG-N-424x (PDX model, Fig. 6A) and NBL-S (cell line xenograft model, Fig. 6B). Because of the absence of overt toxicity in the above models, CDX-0125-TEI was dosed at 15 mg/kg once weekly for two doses and compared with unconjugated CDX-0125 and control IgG1. We observed antitumor activity in both models in the absence of toxicity; objective tumor regressions were seen at early time points in the COG-N-424x PDX model, and a survival advantage was observed in both models (table S3). We again observed abrogation of ALK signaling in NBL-S across a range of doses, although not at 10 mg/kg despite induction of apoptosis (fig. S5). Last, to explore more prolonged exposures to CDX-0125-TEI, we studied weekly dosing at 3 and 10 mg/kg over the course of 4 weeks (fig. S6) and observed tumor shrinkage from enrollment size and further prolongation of survival but eventual escape in all animals after treatment cessation. Collectively, these preclinical models show that CDX-0125-TEI demonstrates robust antitumor activity

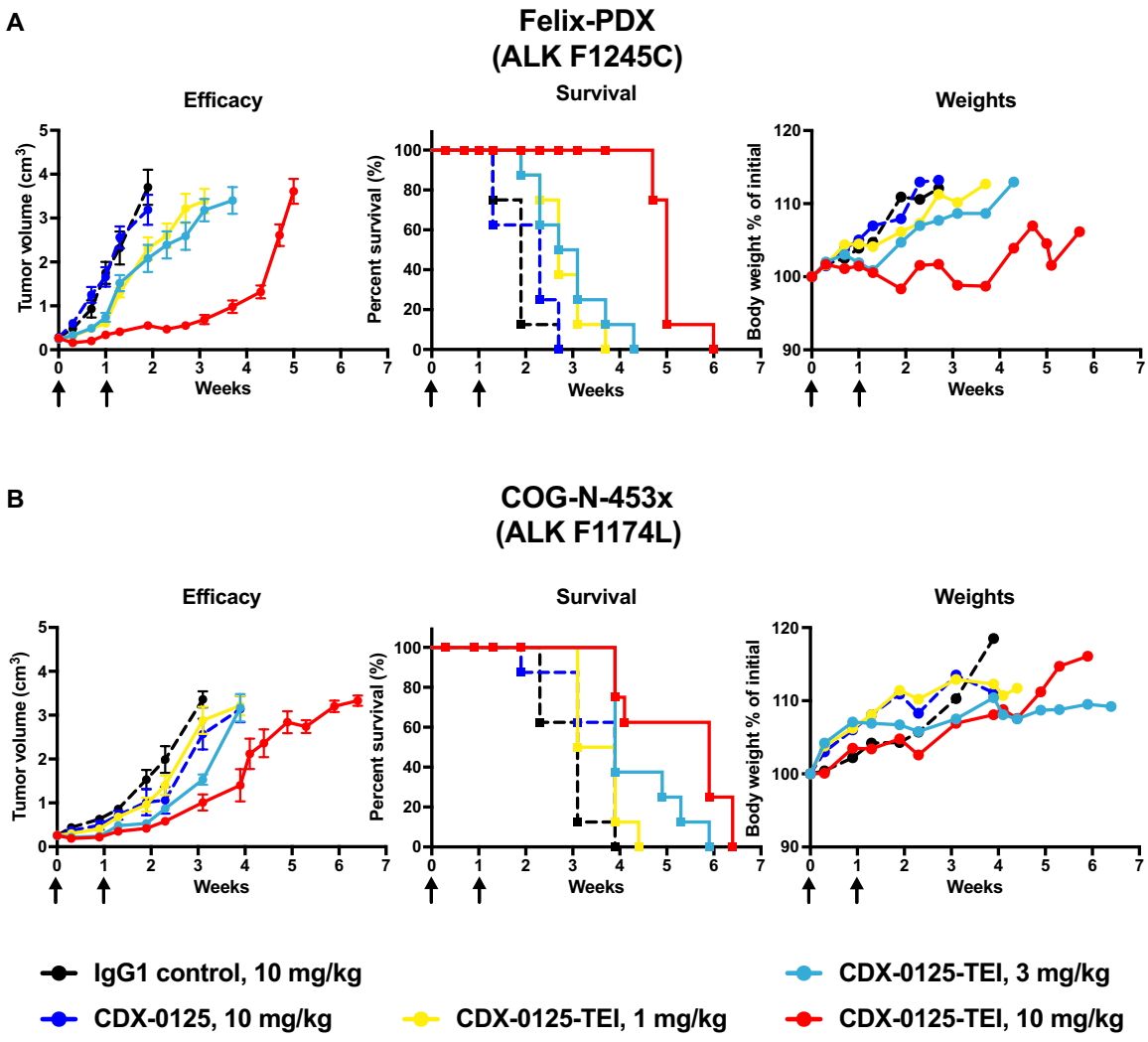

Fig. 5. CDX-0125-TEI induces antitumor activity in ALK mutant PDX models of neuroblastoma. The in vivo efficacy of CDX-0125-TEI was evaluated in female CB17 severe combined immunodeficient (SCID) mice bearing (**A**) Felix-PDX (ALK F1245C) and (**B**) COG-N-453x (ALK F1174L). Upon enrollment, mice (n = 10 per group) were intraperitoneally injected with the following drugs: CDX-0125-TEI [1 mg/kg (yellow), 3 mg/kg (light blue), or 10 mg/kg (red)], IgG control (10 mg/kg) (black), or CDX-0125 (10 mg/kg) (dark blue) on day 0 of enrollment and on day 7, indicated by arrows. Tumor volume was measured twice a week until tumors reached ≥3 cm^3 (left graphs). Kaplan-Meier curves (middle graphs) were compared using a log-rank test and expressed as percentage of survival. Mouse body weight was measured twice a week and expressed as percentage of initial body weight (right graphs).

in ALK-expressing neuroblastoma PDX models, independent of *ALK* mutation status.

DISCUSSION

Targeted therapies that inhibit driver oncogene mutations have the advantage of being highly tumor specific. However, as we have shown for ALK-driven neuroblastomas, only a subset of tumors harbor activating mutations, and primary and/or acquired drug resistance is a major obstacle (*9*, *10*, *12*, *13*, *29*). To be a safe immunotherapeutic target, a cell surface molecule must show absent or very limited cell surface expression on normal human tissues. We have previously shown that ALK is widely expressed in most high-risk primary neuroblastoma tumors regardless of mutation status and that expression is stronger in patients with advanced-stage and *MYCN*-amplified disease (*17*). In this study, we confirm tumor-specific cell surface ALK expression in human neuroblastoma–derived cell lines and PDXs and the absence of expression in pediatric normal tissues.

We generated and tested a panel of ALK antibodies raised against the extracellular domain of ALK and found these reagents to be insufficiently effective at blocking signaling or inducing ADCC to be developed as therapeutic antibodies. A recent study explored the utility of targeting ALK using CAR-based immunotherapy and showed limited antitumor activity (*30*) but used cell line models with low ALK expression; future CAR T cell approaches directed against ALK will require optimization to engage more signaling molecules and testing in relevant ALK-expressing models. Here, we explored the potential of achieving antitumor activity in ALK-expressing neuroblastoma models by conjugating a highly specific ALK antibody (CDX-0125) with a TEI payload that promotes cell death. This approach addresses the challenges of threshold receptor density, which, for ALK, varies substantially. We show that conjugation to a DNA-alkylating agent is much more potent at inducing cytotoxicity in

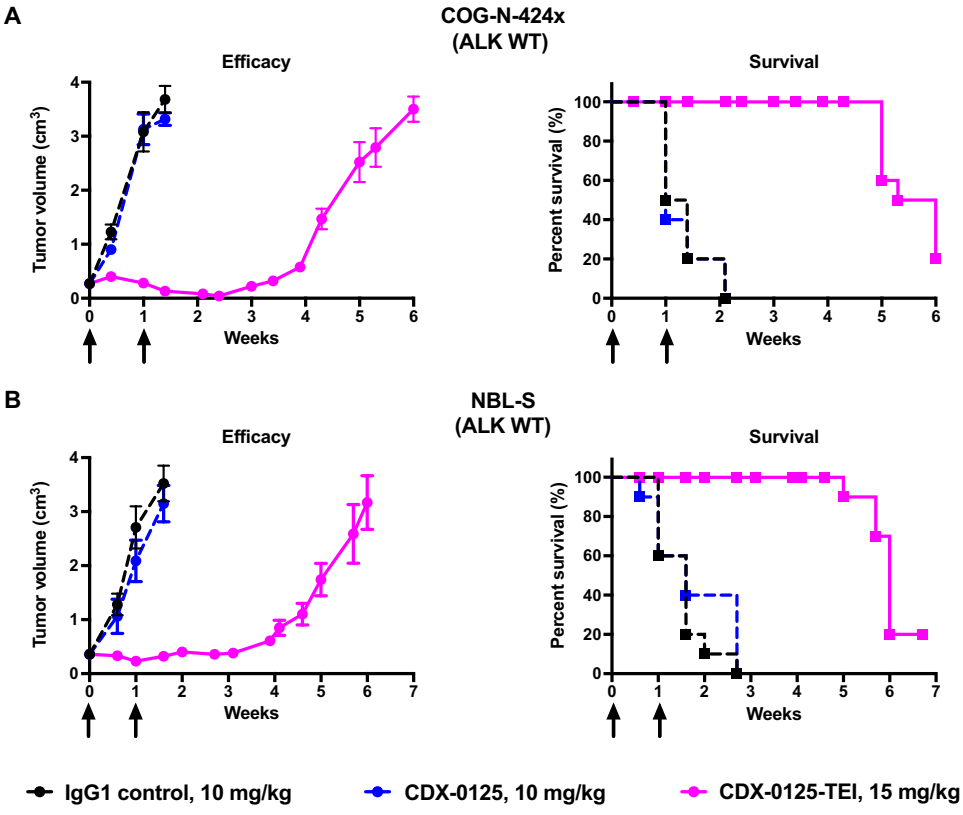

Fig. 6. CDX-0125-TEI induces antitumor activity in ALK wild-type models of neuroblastoma. The in vivo efficacy of CDX-0125-TEI was evaluated in female CB17 SCID mice bearing (**A**) COG-N-424x (ALK wild-type) and (**B**) NBL-S (ALK wild-type). Upon enrollment, mice (n = 10 per group) were intraperitoneally injected with 15 mg/kg of one of the following drugs: CDX-0125-TEI (magenta), IgG control (black), or CDX-0125 (blue) on day 0 of enrollment and on day 7, indicated by arrows. Tumor volume was measured twice a week until tumors reached ≥3 cm^3 (left graphs). Kaplan-Meier curves (right graphs) were compared using a log-rank test and expressed as percentage of survival.

neuroblastoma cells than conjugation with a tubulin-disrupting agent. Our in vitro studies revealed potent antibody binding, effective internalization, selective delivery of the cytotoxic agent, and induction of apoptosis in a panel of human neuroblastoma–derived cell lines with differential ALK expression.

To assess the therapeutic activity of CDX-0125-TEI, we treated PDX models, several of which are generated from heavily pretreated patients with drug-resistant neuroblastoma expressing varying amounts of cell surface ALK. We demonstrated antitumor efficacy only against models with relatively high cell surface ALK expression. We also showed transient down-regulation of activated ALK in vivo, suggesting that if administered consistently, antibody binding could inhibit ALK-mediated cell signaling, whereas the conjugated DNA-alkylating agent provides cytotoxic activity. These preclinical data provide proof of concept that targeting cell surface ALK using an ADC approach is a rational strategy for ALK-expressing neuroblastomas. Future work will need to focus on development of other candidate binders to diverse epitopes, as well as further characterization of the cell surface receptor density threshold required for ADC targeting. We observed that although the expression of cell surface receptor was independent of *ALK* mutation status, modest expression of ALK was not sufficient to elicit ADC-mediated cytotoxicity in vitro and in vivo. We expect that it will be important to determine whether receptor density and intratumoral heterogeneity influence the efficacy of an ALK ADC approach. To address this, we may need to develop a quantitative assay for ALK expression to best select patients for future clinical trials. There are likely other epitope binding sites that could result in higher efficacy, including more efficient internalization and release of toxin in the cytoplasm. In addition, it is possible that our ADC DAR of 2.7 is not sufficient to produce maximally effective antitumor activity, especially in models with low cell surface ALK such as COG-N-453x. The potent effect of free TEI toxin in our in vitro studies pointed to a concentration-dependent mechanism of action of free TEIs and suggests that further development of an ADC with a higher DAR could be beneficial, although several studies have shown that a higher DAR can promote poor pharmacokinetic properties, antibody fragmentation and aggregation, and increased off-target toxicity (*31*).

These data show that ALK is a suitable target for an ADC approach, which can broaden the utility of this target in neuroblastoma and other ALK-expressing malignancies (*32*). The clinical development of an ALK ADC approach, which should be safe because of the absence of ALK expression on normal tissues, will require human studies and retrospective quantification of ALK expression in patient tumors to inform whether a target expression cutoff can predict improved efficacy and duration of responses.

MATERIALS AND METHODS

Study design

This study was designed to develop immune-targeting strategies against the native ALK protein expressed on the cell surface of neuroblastoma tumors. An IHC assay using a commercially available anti-ALK mAb was optimized to evaluate ALK expression on a panel of 32 PDXs from high-risk human primary tumors in TMAs and showed that ALK is widely expressed on the cell surface of most neuroblastoma tumors and its expression appears to be restricted to tumor tissue. A panel of 32 ALK-targeting mAbs was generated by immunizing mice with a purified human ALK antigen encompassing the extracellular domain, with prioritization of nine antibodies for further testing. None of the candidate naked antibodies exhibited antiproliferative activity, nor could they induce an immune-mediated antitumor response in neuroblastoma cell lines. mAb CDX-0125 was selected as an appropriate candidate for further evaluation, including quantification of plasma membrane ALK expression using flow cytometry in a panel of human neuroblastoma–derived cell lines and assessment of internalization kinetics. Flow cytometry showed

highly variable ALK expression with no correlation to underlying ALK mutation status. The extent of CDX-0125 internalization in each cell line differed considerably and was proportional to the magnitude of cell surface ALK expression. An ALK ADC (CDX-0125-TEI) was generated by the conjugation of purified CDX-0125 to the TEI derivative NMS-P945, a DNA minor groove alkylating agent bearing a peptidic cleavable drug linker and a self-immolative spacer. The cytotoxic activity of CDX-0125-TEI against a panel of four human neuroblastoma–derived cell lines expressing different forms and amounts of cell surface ALK was evaluated using cell viability assays conducted with multiple technical and biological replicates to ensure reproducibility of data. To evaluate the in vivo antitumor activity of an ALK-ADC, we conducted pilot testing across a range of doses in neuroblastoma xenograft models harboring varying ALK expression and mutation status. Sample size (n = 10) was chosen on the basis of power analysis to be sufficient to define statistically significant differences in tumor response rates between each treatment arm. Data collection was ceased, and the mice were euthanized if they showed ≥20% weight loss from their initial body weight or when their tumor volume reached ≥3 cm^3. Mice were randomized to control versus treatment groups, and the investigators were not blinded to the experiments.

mAb generation

The region of human ALK encompassing the glycine-rich region and epidermal growth factor domain (T637-S1038) was expressed as a His-tagged protein in 293-F cells, purified by nickel affinity chromatography, and buffer-exchanged to phosphate-buffered saline (PBS). Mouse immunizations and hybridoma generation were carried out by Abpro Therapeutics. Hybridomas yielding ALK-reactive mAbs were subcloned to ensure monoclonality. Variable heavy and light regions from hybridomas of interest were amplified by rapid amplification of complementary DNA ends (RACE) and subcloned into vectors containing human IgG1 constant heavy or light domains to generate chimeric antibodies. Purified chimeric antibodies were functionally tested to ensure similar activity to the hybridoma-derived mouse mAb.

Antibody purification and ADC conjugation

A subset of 32 antibodies against both the C-terminal and the N-terminal portions of ALK protein were purified from the conditioned media of subcloned hybridomas. Hybridomas were grown in serum-free hybridoma medium (Invitrogen) supplemented with 2% super low IgG fetal bovine serum (FBS) (HyClone), and the ALK IgG in the conditioned supernatant was purified over protein G. The antibodies were eluted with acid, immediately neutralized, and buffer-exchanged into PBS. Typical purity was >95%. The antibody concentrations were determined by A_{280} (absorbance at 280 nm), and quality (% aggregation and purity) was assessed by size exclusion chromatography–ultra-performance liquid chromatography (SEC-UPLC).

Plasmids encoding the light and heavy chain of CDX-0125 or a control human IgG1 chimeric antibody were transiently coexpressed in Expi293 cells (Thermo Fisher Scientific) using polyethylenimine. Conditioned medium containing the antibodies was flowed over a MabSelect SuRe column (GE Healthcare). Bound antibody was washed with PBS, eluted in 0.1 M glycine (pH 2.7), and immediately neutralized with 1 M tris (pH 7.4). Purified antibody was buffer-exchanged into PBS by tangential flow filtration using a Sartorius Slice ECO with a 30-kDa cutoff Hydrosart cassette. The antibody was purified with low endotoxin (<1 endotoxin unit/mg) and was >95% pure and >95% monomeric, as assessed by SDS–polyacrylamide gel electrophoresis (SDS-PAGE) and SEC-UPLC using a UPLC BEH200 column in a Waters Acquity instrument.

Hybridomas expressing anti-ALK mAbs were established from mice immunized with fragments of the purified ALK extracellular domain (Abpro Therapeutics). Binding of each mAb to ALK-expressing neuroblastoma cells was confirmed by flow cytometry. Among these, CDX-0125 was selected on the basis of its cross-species reactivity, affinity, and cytotoxic activity in ALK-positive neuroblastoma cells when conjugated to the TEI payload NMS-P945. CDX-0125 was converted to a human IgG1 bearing human constant light and heavy chains and murine variable domains.

NMS-P945 was conjugated to the CDX-0125 antibody through a partial interchain disulfide reduction followed by derivatization with the drug with the aim of reaching an average DAR of 2.5 to 3.0. The resulting ADC CDX-0125-TEI was characterized by SEC to check for aggregated material, by hydrophobic interaction chromatography to evaluate the distribution of the different isoforms, and by reducing and nonreducing SDS-PAGE to assess purity. Liquid chromatography–mass spectrometry analysis on the reduced product allowed DAR determination.

Antibody-dependent cell-mediated cytotoxicity

ADCC assays were performed using peripheral blood mononuclear cells (PBMCs) from de-identified normal healthy donors as effectors. PBMCs were obtained from the Children's Hospital of Philadelphia Core Facility. Target cells were preincubated with the control IgG1 mAb, CDX-0125, or the anti-GD2 ch14.18 mAb (1, 10, and 25 μg/ml) for 1 hour before mixing with PBMCs and incubated for an additional 4 hours at a 50:1 effector/target cell ratio. ADCC was measured as a function of intracellular release of endogenous GAPDH using an aCella-TOX kit (Cell Technology Inc.).

Binding assays

CDX-0125 binding assays were performed on cells expressing human (NB-1) and mouse (Neuro-2a) ALK. The ALK-null cell line SK-N-AS was used as negative control. Briefly, cells were lifted with EDTA, blocked for 1 hour on ice in PBE (PBS containing 0.2% IgG-free bovine serum albumin and 2 mM EDTA), and subsequently incubated with increasing concentrations of CDX-0125 in PBE for 2 hours on ice. Cells were washed and incubated with a goat anti-human secondary antibody labeled with Alexa Fluor 647 (Jackson ImmunoResearch) for 1 hour on ice. Cells were washed, incubated with 7-aminoactinomycin D (7-AAD) to gate out dead cells, and read in an Accuri C6 flow cytometer (BD Biosciences). Background-subtracted mean fluorescence intensities were normalized and plotted as a function of antibody concentration. Data were fit to a single binding site equation using GraphPad Prism, from which apparent K_d values were derived.

Internalization

Cell-based antibody binding and internalization were quantitatively assessed by flow cytometry, as described in (*33*). Briefly, cells were preincubated with CDX-0125 (100 nM) at 4°C for 30 min to allow binding to occur. After a wash step, cells were incubated in an atmosphere of 5% CO_2 at 37°C for the indicated time intervals ranging from 10 to 60 min (triplicates). Cells collected from each of these time points were next incubated with an anti-human IgG Fc PE antibody (Invitrogen). Internalized CDX-0125 was represented

by absolute fluorescence units obtained by subtracting fluorescence of cells incubated at different time points from fluorescence of cells kept at 4°C—a condition that halted internalization. Microscopy-based assessment of antibody internalization was performed in NB-1 cells plated in coverslips. Qualitative analysis was achieved by microscopic inspection of green fluorescence using the 488-nm laser channel (Leica CTR5000, LAS X) in cells incubated with Alexa 488–labeled CDX-0125 at 4°C for 30 min and at 37°C, 5% CO_2 for 4 hours.

Cell viability assays

Cells were seeded at 2000 cells per well in black 96-well proliferation plates (Corning) and dosed with a titration of conjugates or free toxin (NMS-P528) for 3 to 5 days, until control untreated cells reached 80 to 90% confluence. Cytotoxicity was measured with CellTiter-Glo (Promega) using a Synergy HT plate reader (BioTek). Luminescence values were entered into GraphPad Prism and plotted as a function of drug concentration. Data were fit to a four-parameter nonlinear regression algorithm and normalized to control treatment, from which IC_{50} values were derived.

Single-strand DNA damage analysis

Cells were treated with either IgG1 controls or CDX-0125-TEI for 5 days and further analyzed upon overnight fixation in methanol/PBS (6:1). Staining with F7-26 mAb was performed and analyzed with an LSR II flow cytometer (BD Biosciences), and data were acquired using microspheres labeled with predetermined amounts of Alexa 488 (Bangs Laboratories Inc.). The beads were run in parallel with samples to establish a calibration curve relating instrument channel values and standardized fluorescence intensity units.

Apoptosis

The relative percentage of apoptotic cells were assessed using the Annexin V-FITC Apoptosis Detection Kit (BD Pharmingen), according to the manufacturer's protocol. Briefly, cells were washed twice with PBS, and the pellet was resuspended in annexin V binding buffer at a concentration of about 10^6 per milliliter. Five microliters of annexin V–FITC per 10^5 cells was added to the samples. Tubes were incubated for 15 min at room temperature in the dark before FACS analysis.

Immunoblot analysis of protein expression

Phosphorylated/total ALK and markers of apoptosis were measured by Western blotting 5 days after dosing, as previously described (*13*). Briefly, total protein concentration was measured using the bicinchoninic acid (BCA) method, and 50 or 150 μg of protein in cells or tissues, respectively, was separated on 4 to 12% bis-tris gradient gels. Upon immobilization onto polyvinylidene difluoride (PVDF) membranes, proteins were labeled using one of the following antibodies: phosphorylated ALK (Y1278), total ALK, cleaved caspase-3, and GAPDH (Cell Signaling Technology). Subsequently, membranes were washed with tris-buffered saline with Tween-20 (TBST), incubated with horseradish peroxidase (HRP)–conjugated secondary antibodies, and developed using Pierce SuperSignal West Femto Maximum Sensitivity Substrate (Thermo Scientific).

TMA construction

PDX-bearing mice were euthanized when the tumor reached 0.6 to 1.5 cm^3 in volume. Tissue was fixed in 10% neutral buffered formalin (Thermo Scientific, catalog no. 9400-1) and paraffin-embedded. Blocks were sectioned, and hematoxylin and eosin (H&E) staining was performed to obtain a template guide slide to match the face of each tissue block. A finalized list of tissue blocks for each array was then used to create a final PDX TMA map in the Galileo TMA software package (Integrated Systems Engineering S.r.l.). Briefly, the array was designed using 0.6-mm punches, and each tissue was punched at least in duplicate. In instances where more than one PDX sample was available for a given model, we included two tumors from two separate mice for each model (four cores total per model, two punches from two separate tumors). A total of 144 PDX cores were used in each TMA block. Human placenta was used as an orientation marker on each array to mark the starting point (upper left-hand corner) and also a row down the middle of each sector to aid in manual reading of the array. Using the marked slides as a guide, core biopsies (0.6 mm) were extracted from the donor blocks and inserted into the recipient block at defined array coordinates. After punching, TMA blocks were heated in a 60°C oven for 5 to 10 min, and a blank slide was used to level the face of the TMA block. The normal pediatric TMA for ALK expression was previously reported (*6*).

Immunohistochemistry

IHC with rabbit anti-ALK clone D5F3 (Cell Signaling, catalog no. 3633) antibody was performed using a Bond Max automated staining system (Leica Biosystems. DS9263). Avidin/Biotin solution (Vector Labs, SP-2001) and Protein Block (Dako, X0909) were added. Anti-ALK antibody was used at 1:500 dilution, and antigen retrieval was performed with E2 (Leica Microsystems) retrieval solution for 20 min. Slides were rinsed, dehydrated through a series of ascending concentrations of ethanol and xylene, and then coverslipped. Stained slides were then digitally scanned on an Aperio CSO slide scanner (Leica Biosystems). The expression of ALK was evaluated using H-scores. The H-scores consisted of an assessment of the intensity of staining and the percentage of the staining area having a given intensity. Only stained malignant cells were assessed. The samples were grouped into the following four categories based on the intensity of nuclear staining: none (0), weak (1), medium (2), and strong (3). The indexed sum was obtained by multiplying the intensity grade by the percentage of staining area.

Quantitation of ALK cell surface number

ALK cell surface number was determined using a flow cytometry–based QIFIKIT assay (Dako/Agilent), according to the manufacturer's instructions. Briefly, cultured neuroblastoma cells were detached using 2 mM EDTA in PBS and blocked in FACS buffer [PBS with 1% FBS (HyClone)] for 1 hour on ice. Cells were treated with 50 nM of the fully murine precursor of mAb CDX-0125 for 1 hour on ice, washed in FACS buffer, and stained with an FITC-labeled anti-mouse secondary antibody provided with the kit. Cells were washed in FACS buffer and incubated with 7-AAD for 5 min to exclude dead cells, and fluorescence was measured using an Accuri C6 flow cytometer (BD Biosciences). Receptor number was determined by interpolating measured cell fluorescence to calibration standards provided in the kit, as described by the manufacturer.

PDX dissociation

Freshly dissected tumor tissues were dissociated into single-cell suspensions using the Tumor Dissociation Kit (MACS Miltenyi Biotec). Briefly, the tumor tissue was enzymatically digested using the kit components and the gentleMACS Dissociators for mechanical dissociation

steps (*34*). After dissociation, samples were applied to a filter to remove any remaining larger particles from the single-cell suspension. Subsequently, samples were centrifuged for 5 min at 300*g*, and pellets containing red blood cells were incubated with Red Blood Cell Lysis Solution (MACS Miltenyi Biotec). Remaining tumor cells (2×10^6) were incubated with magnetic beads to remove mouse stroma cells (Mouse Cell Depletion Kit, MACS Miltenyi Biotec) and then passed through magnetic columns to retain bound mouse cells. Collected fractions containing pure human tumor cells were immediately used for flow cytometry and immunoblotting analyses.

Flow cytometry

Cells were plated at about 80% density 1 day before flow cytometry analysis. Cells were kept ice-cold during staining to prevent receptor internalization. Cells were harvested, washed, and then incubated with unconjugated ALK antibody CDX-0125 at 100 nM final concentration in PBS with 2% FBS for 1 hour. After three washes, cells were incubated with a goat F(ab′) anti-human IgG PE conjugate (Invitrogen) for 30 min. Cells were run on an LSR II flow cytometer (BD Biosciences). Data were analyzed using FlowJo software, and mean fluorescence was determined using standard PE beads (Bangs Laboratories Inc.). All results shown are representative of at least three independent experiments. Flow cytometry analysis in dissociated tumors was carried out using a commercially available ALK antibody (D5F3, Cell Signaling) following the same protocol used for cell line staining.

In vivo efficacy studies

All studies were approved by the Children's Hospital of Philadelphia Institutional Animal Care and Use Committee protocol no. IAC 000643. Felix, COG-N-424x, and COG-N-453x PDXs and the NBL-S cell line–derived xenograft were implanted subcutaneously into the right flanks of female CB17 SCID female mice. When tumors reached 200 mm^3, the animals were randomized into groups of 10 and dosed intraperitoneally for two consecutive weeks—total of two single injections—with the indicated treatments (IgG: 10 mg/kg, CDX-0125: 10 mg/kg, or CDX-0125-TEI: 1, 3, or 10 mg/kg). In some models, animals were treated with four injections of 10 mg/kg or two injections of 15 mg/kg of CDX-0125-TEI or vehicle in consecutive weeks. Tumor volume [spheroid formula: V (volume in cm^3) = $((L/2 + W/2)\text{^}3*\pi/6)/1000$, where L = length and W = width] and total body weight were recorded two to three times weekly. Mice were euthanized via carbon dioxide inhalation from a compressed gas cylinder at tumor size ≥ 3 cm^3. Death was ensured by cervical dislocation after cessation of breathing as a secondary method of euthanasia.

Statistical analysis

A linear mixed-effects model was used to test the difference in the rate of tumor volume change over time among different groups. Survival percentages were estimated using Kaplan-Meier methods, and survival curves were compared using the log-rank test. Primary data are shown in data file S1.

SUPPLEMENTARY MATERIALS

www.sciencetranslationalmedicine.org/cgi/content/full/11/483/eaau9732/DC1

Fig. S1. Unconjugated anti-ALK mAbs do not elicit cytotoxic activity alone or as mediators of ADCC.
Fig. S2. ALK is expressed in neuroblastoma but not in normal pediatric tissues.
Fig. S3. The DNA-alkylating CDX-0125-TEI is more potent than the CDX-0125-tubulin inhibitor.
Fig. S4. CDX-0125-TEI induces single-strand DNA damage.
Fig. S5. CDX-0125-TEI down-regulates phosphorylated ALK in treated PDXs and cell line xenografts.
Fig. S6. Weekly dosing with CDX-0125-TEI shows potent but transient antitumor activity in the ALK wild-type NBL-S xenograft model.
Table S1. List of screened ALK mAbs.
Table S2. Statistical analysis for in vivo efficacy studies in Felix, NBL-S, and COG-N-453x.
Table S3. Statistical analysis for in vivo efficacy studies in COG-N-424x and NBL-S.
Data file S1. Primary data.

REFERENCES AND NOTES

1. T. J. Pugh, O. Morozova, E. F. Attiyeh, S. Asgharzadeh, J. S. Wei, D. Auclair, S. L. Carter, K. Cibulskis, M. Hanna, A. Kiezun, J. Kim, M. S. Lawrence, L. Lichenstein, A. McKenna, C. S. Pedamallu, A. H. Ramos, E. Shefler, A. Sivachenko, C. Sougnez, C. Stewart, A. Ally, I. Birol, R. Chiu, R. D. Corbett, M. Hirst, S. D. Jackman, B. Kamoh, A. H. Khodabakshi, M. Krzywinski, A. Lo, R. A. Moore, K. L. Mungall, J. Qian, A. Tam, N. Thiessen, Y. Zhao, K. A. Cole, M. Diamond, S. J. Diskin, Y. P. Mosse, A. C. Wood, L. Ji, R. Sposto, T. Badgett, W. B. London, Y. Moyer, J. M. Gastier-Foster, M. A. Smith, J. M. G. Auvil, D. S. Gerhard, M. D. Hogarty, S. J. M. Jones, E. S. Lander, S. B. Gabriel, G. Getz, R. C. Seeger, J. Khan, M. A. Marra, M. Meyerson, J. M. Maris, The genetic landscape of high-risk neuroblastoma. *Nat. Genet.* **45**, 279–284 (2013).
2. K. R. Bosse, J. M. Maris, Advances in the translational genomics of neuroblastoma: From improving risk stratification and revealing novel biology to identifying actionable genomic alterations. *Cancer* **122**, 20–33 (2016).
3. A. L. Yu, A. L. Gilman, M. F. Ozkaynak, W. B. London, S. G. Kreissman, H. X. Chen, M. Smith, B. Anderson, J. G. Villablanca, K. K. Matthay, H. Shimada, S. A. Grupp, R. Seeger, C. P. Reynolds, A. Buxton, R. A. Reisfeld, S. D. Gillies, S. L. Cohn, J. M. Maris, P. M. Sondel, Children's Oncology Group, Anti-GD2 antibody with GM-CSF, interleukin-2, and isotretinoin for neuroblastoma. *N. Engl. J. Med.* **363**, 1324–1334 (2010).
4. D. W. Lee, J. N. Kochenderfer, M. Stetler-Stevenson, Y. K. Cui, C. Delbrook, S. A. Feldman, T. J. Fry, R. Orentas, M. Sabatino, N. N. Shah, S. M. Steinberg, D. Stroncek, N. Tschernia, C. Yuan, H. Zhang, L. Zhang, S. A. Rosenberg, A. S. Wayne, C. L. Mackall, T cells expressing CD19 chimeric antigen receptors for acute lymphoblastic leukaemia in children and young adults: A phase 1 dose-escalation trial. *Lancet* **385**, 517–528 (2015).
5. S. L. Maude, N. Frey, P. A. Shaw, R. Aplenc, D. M. Barrett, N. J. Bunin, A. Chew, V. E. Gonzalez, Z. Zheng, S. F. Lacey, Y. D. Mahnke, J. J. Melenhorst, S. R. Rheingold, A. Shen, D. T. Teachey, B. L. Levine, C. H. June, D. L. Porter, S. A. Grupp, Chimeric antigen receptor T cells for sustained remissions in leukemia. *N. Engl. J. Med.* **371**, 1507–1517 (2014).
6. K. R. Bosse, P. Raman, Z. Zhu, M. Lane, D. Martinez, S. Heitzeneder, K. S. Rathi, N. M. Kendsersky, M. Randall, L. Donovan, S. Morrissy, R. T. Sussman, D. V. Zhelev, Y. Feng, Y. Wang, J. Hwang, G. Lopez, J. L. Harenza, J. S. Wei, B. Pawel, T. Bhatti, M. Santi, A. Ganguly, J. Khan, M. A. Marra, M. D. Taylor, D. S. Dimitrov, C. L. Mackall, J. M. Maris, Identification of GPC2 as an oncoprotein and candidate immunotherapeutic target in high-risk neuroblastoma. *Cancer Cell* **32**, 295–309.e12 (2017).
7. Y. P. Mossé, M. Laudenslager, L. Longo, K. A. Cole, A. Wood, E. F. Attiyeh, M. J. Laquaglia, R. Sennett, J. E. Lynch, P. Perri, G. Laureys, F. Speleman, C. Kim, C. Hou, H. Hakonarson, A. Torkamani, N. J. Schork, G. M. Brodeur, G. P. Tonini, E. Rappaport, M. Devoto, J. M. Maris, Identification of *ALK* as a major familial neuroblastoma predisposition gene. *Nature* **455**, 930–935 (2008).
8. I. Janoueix-Lerosey, D. Lequin, L. Brugières, A. Ribeiro, L. de Pontual, V. Combaret, V. Raynal, A. Puisieux, G. Schleiermacher, G. Pierron, D. Valteau-Couanet, T. Frebourg, J. Michon, S. Lyonnet, J. Amiel, O. Delattre, Somatic and germline activating mutations of the ALK kinase receptor in neuroblastoma. *Nature* **455**, 967–970 (2008).
9. S. C. Bresler, D. A. Weiser, P. J. Huwe, J. H. Park, K. Krytska, H. Ryles, M. Laudenslager, E. F. Rappaport, A. C. Wood, P. W. McGrady, M. D. Hogarty, W. B. London, R. Radhakrishnan, M. A. Lemmon, Y. P. Mossé, *ALK* mutations confer differential oncogenic activation and sensitivity to *ALK* inhibition therapy in neuroblastoma. *Cancer Cell* **26**, 682–694 (2014).
10. S. C. Bresler, A. C. Wood, E. A. Haglund, J. Courtright, L. T. Belcastro, J. S. Plegaria, K. Cole, Y. Toporovskaya, H. Zhao, E. L. Carpenter, J. G. Christensen, J. M. Maris, M. A. Lemmon, Y. P. Mossé, Differential inhibitor sensitivity of anaplastic lymphoma kinase variants found in neuroblastoma. *Sci. Transl. Med.* **3**, 108ra114 (2011).
11. R. E. George, T. Sanda, M. Hanna, S. Fröhling, W. Luther II, J. Zhang, Y. Ahn, W. Zhou, W. B. London, P. McGrady, L. Xue, S. Zozulya, V. E. Gregor, T. R. Webb, N. S. Gray, D. G. Gilliland, L. Diller, H. Greulich, S. W. Morris, M. Meyerson, A. T. Look, Activating mutations in ALK provide a therapeutic target in neuroblastoma. *Nature* **455**, 975–978 (2008).
12. N. R. Infarinato, J. H. Park, K. Krytska, H. T. Ryles, R. Sano, K. M. Szigety, Y. Li, H. Y. Zou, N. V. Lee, T. Smeal, M. A. Lemmon, Y. P. Mossé, The ALK/ROS1 inhibitor PF-06463922 overcomes primary resistance to crizotinib in ALK-driven neuroblastoma. *Cancer Discov.* **6**, 96–107 (2016).
13. K. Krytska, H. T. Ryles, R. Sano, P. Raman, N. R. Infarinato, T. D. Hansel, M. R. Makena, M. M. Song, C. P. Reynolds, Y. P. Mossé, Crizotinib synergizes with chemotherapy in preclinical models of neuroblastoma. *Clin. Cancer Res.* **22**, 948–960 (2016).

14. Y. P. Mossé, M. S. Lim, S. D. Voss, K. Wilner, K. Ruffner, J. Laliberte, D. Rolland, F. M. Balis, J. M. Maris, B. J. Weigel, A. M. Ingle, C. Ahern, P. C. Adamson, S. M. Blaney, Safety and activity of crizotinib for paediatric patients with refractory solid tumours or anaplastic large-cell lymphoma: A Children's Oncology Group phase 1 consortium study. *Lancet Oncol.* **14**, 472–480 (2013).
15. Y. P. Mossé, S. D. Voss, M. S. Lim, D. Rolland, C. G. Minard, E. Fox, P. Adamson, K. Wilner, S. M. Blaney, B. J. Weigel, Targeting ALK with crizotinib in pediatric anaplastic large cell lymphoma and inflammatory myofibroblastic tumor: A Children's Oncology Group study. *J. Clin. Oncol.* **35**, 3215–3221 (2017).
16. A. C. Wood, K. Krytska, H. T. Ryles, N. R. Infarinato, R. Sano, T. D. Hansel, L. S. Hart, F. J. King, T. R. Smith, E. Ainscow, K. B. Grandinetti, T. Tuntland, S. Kim, G. Caponigro, Y. Q. He, S. Krupa, N. Li, J. L. Harris, Y. P. Mossé, DualALKandCDK4/6Inhibition demonstrates synergy against neuroblastoma. *Clin. Cancer Res.* **23**, 2856–2868 (2017).
17. E. L. Carpenter, E. A. Haglund, E. M. Mace, D. Deng, D. Martinez, A. C. Wood, A. K. Chow, D. A. Weiser, L. T. Belcastro, C. Winter, S. C. Bresler, M. Vigny, P. Mazot, S. Asgharzadeh, R. C. Seeger, H. Zhao, R. Guo, J. G. Christensen, J. S. Orange, B. R. Pawel, M. A. Lemmon, Y. P. Mossé, Antibody targeting of anaplastic lymphoma kinase induces cytotoxicity of human neuroblastoma. *Oncogene* **31**, 4859–4867 (2012).
18. J. Guan, G. Umapathy, Y. Yamazaki, G. Wolfstetter, P. Mendoza, K. Pfeifer, A. Mohammed, F. Hugosson, H. Zhang, A. W. Hsu, R. Halenbeck, B. Hallberg, R. H. Palmer, FAM150A and FAM150B are activating ligands for anaplastic lymphoma kinase. *eLife* **4**, e09811 (2015).
19. A. V. Reshetnyak, P. B. Murray, X. Shi, E. S. Mo, J. Mohanty, F. Tome, H. Bai, M. Gunel, I. Lax, J. Schlessinger, Augmentor α and β (FAM150) are ligands of the receptor tyrosine kinases ALK and LTK: Hierarchy and specificity of ligand-receptor interactions. *Proc. Natl. Acad. Sci. U.S.A.* **112**, 15862–15867 (2015).
20. M. X. Sliwkowski, I. Mellman, Antibody therapeutics in cancer. *Science* **341**, 1192–1198 (2013).
21. B. A. Teicher, R. V. Chari, Antibody conjugate therapeutics: Challenges and potential. *Clin. Cancer Res.* **17**, 6389–6397 (2011).
22. A. Thomas, B. A. Teicher, R. Hassan, Antibody-drug conjugates for cancer therapy. *Lancet Oncol.* **17**, e254–e262 (2016).
23. M. Caruso, Thienoindoles: New highly promising agents for antibody drug conjugates generation, in *Proceedings of the 109th Annual Meeting of the American Association for Cancer Research*, Chicago, IL, 14 to 18 April 2018.
24. B. H. Kushne, N. K. Cheung, GM–CSF enhances 3F8 monoclonal antibody-dependent cellular cytotoxicity against human melanoma and neuroblastoma. *Blood* **73**, 1936–1941 (1989).
25. J. A. Hank, R. R. Robinson, J. Surfus, B. M. Mueller, R. A. Reisfeld, N.-K. Cheung, P. M. Sondel, Augmentation of antibody dependent cell mediated cytotoxicity following in vivo therapy with recombinant interleukin 2. *Cancer Res.* **50**, 5234–5239 (1990).
26. S. Tanqri, H. Vall, D. Kaplan, B. Hoffman, N. Purvis, A. Porwit, B. Hunsberger, T. V. Shankey, on behalf of ICSH/ICCS Working Group, Validation of cell-based fluorescence assays: Practice guidelines from the ICSH and ICCS - part III - analytical issues. *Cytometry B Clin. Cytom.* **84**, 291–308 (2013).
27. B. Valsasina, F. Gasparri, I. Beria, N. Colombo, P. Orsini, R. Perego, S. Rizzi, U. Cucchi, C. Albanese, A. Marsiglio, I. Fraietta, M. Ciomei, S. Cribioli, C. Visco, E. R. Felder, A. Isacchi, E. A. Pesenti, A. Galvani, D. Donati, M. Caruso, Abstract 822: Thienoindoles, a novel class of DNA minor groove alkylating agents highly suited for the generation of novel antibody drug conjugates (ADCs). *Cancer Res.* **74**, 822 (2014).
28. R. S. Grigoryan, B. Yang, N. Keshelava, J. R. Barnhart, C. P. Reynolds, Flow cytometry analysis of single-strand DNA damage in neuroblastoma cell lines using the F7-26 monoclonal antibody. *Cytometry A* **71**, 951–960 (2007).
29. L. S. Hart, J. Rader, P. Raman, V. Batra, M. R. Russell, M. Tsang, M. Gagliardi, L. Chen, D. Martinez, Y. Li, A. Wood, S. Kim, S. Parasuraman, S. Delach, K. A. Cole, S. Krupa, M. Boehm, M. Peters, G. Caponigro, J. M. Maris, Preclinical therapeutic synergy of MEK1/2 and CDK4/6 inhibition in neuroblastoma. *Clin. Cancer Res.* **23**, 1785–1796 (2017).
30. A. J. Walker, R. G. Majzner, L. Zhang, K. Wanhainen, A. H. Long, S. M. Nguyen, P. Lopomo, M. Vigny, T. J. Fry, R. J. Orentas, C. L. Mackall, Tumor antigen and receptor densities regulate efficacy of a chimeric antigen receptor targeting anaplastic lymphoma kinase. *Mol. Ther.* **25**, 2189–2201 (2017).
31. X. Sun, J. F. Ponte, N. C. Yoder, R. Laleau, J. Coccia, L. Lanieri, Q. Qiu, R. Wu, E. Hong, M. Bogalhas, L. Wang, L. Dong, Y. Setiady, E. K. Maloney, O. Ab, X. Zhang, J. Pinkas, T. A. Keating, R. Chari, H. K. Erickson, J. M. Lambert, Effects of drug–antibody ratio on pharmacokinetics, biodistribution, efficacy, and tolerability of antibody–maytansinoid conjugates. *Bioconjug. Chem.* **28**, 1371–1381 (2017).
32. Y. P. Mossé, Anaplastic lymphoma kinase as a cancer target in pediatric malignancies. *Clin. Cancer Res.* **22**, 546–552 (2016).
33. L. R. Saunders, A. J. Bankovich, W. C. Anderson, M. A. Aujay, S. Bheddah, K. A. Black, R. Desai, P. A. Escarpe, J. Hampl, A. Laysang, D. Liu, J. Lopez-Molina, M. Milton, A. Park, M. A. Pysz, H. Shao, B. Slingerland, M. Torgov, S. A. Williams, O. Foord, P. Howard, J. Jassem, A. Badzio, P. Czapiewski, D. H. Harpole, A. Dowlati, P. P. Massion, W. D. Travis, M. C. Pietanza, J. T. Poirier, C. M. Rudin, R. A. Stull, S. J. Dylla, A DLL3-targeted antibody-drug conjugate eradicates high-grade pulmonary neuroendocrine tumor-initiating cells in vivo. *Sci. Transl. Med.* **7**, 302ra136 (2015).
34. V. E. Schneeberger, V. Allaj, E. E. Gardner, J. T. Poirier, C. M. Rudin, Quantitation of murine stroma and selective purification of the human tumor component of patient-derived xenografts for genomic analysis. *PLOS ONE* **11**, e0160587 (2016).

Acknowledgments: We thank our collaborators from Kolltan Pharmaceuticals Inc. (G. McMahon, J. Schlessinger, G. F. Ligon, and J. S. Lillquist) for antibody production. We also acknowledge M. Lemmon (Yale University) for initial concept contribution and valuable suggestions. **Funding:** This work was supported by DoD award W81XWH-12-1-0486, Kolltan Pharmaceuticals, Solving Kids' Cancer, and Braden's Hope Foundation. **Author contributions:** R.S., K.K., D.A., and Y.P.M. contributed to the conception of the work, designed and performed experiments, analyzed data, and drafted the figures and manuscript. C.E.L. performed the in vivo studies. P.R. performed statistical analysis of in vivo studies. D.M. and B.R.P. performed and analyzed the IHC experiments. G.F.L., J.S.L., and D.A. developed the anti-ALK antibodies for testing. U.C., P.O., and S.R. conjugated the ALK antibody using their proprietary linker and toxin technology. **Competing interests:** D.A., G.F.L., and J.S.L. are inventors on patent application WO 2017/035430 held by Celldex Therapeutics that covers anti-ALK antibodies and methods of use thereof. All other authors declare that they have no competing interests. **Data and materials availability:** All data associated with this study are present in the paper or Supplementary Materials. mAbs 4G7, 8A6, 8G7, 8H8, 7F2, 8G10, 2F5, 8D4, and 7C1 and ADCs are available from Y.P.M. under material transfer agreement with the Children's Hospital of Philadelphia.

Submitted 3 August 2018
Accepted 8 January 2019
Published 13 March 2019
10.1126/scitranslmed.aau9732

Citation: R. Sano, K. Krytska, C. E. Larmour, P. Raman, D. Martinez, G. F. Ligon, J. S. Lillquist, U. Cucchi, P. Orsini, S. Rizzi, B. R. Pawel, D. Alvarado, Y. P. Mossé, An antibody-drug conjugate directed to the ALK receptor demonstrates efficacy in preclinical models of neuroblastoma. *Sci. Transl. Med.* **11**, eaau9732 (2019).

Science Translational Medicine

An antibody-drug conjugate directed to the ALK receptor demonstrates efficacy in preclinical models of neuroblastoma

Renata Sano, Kateryna Krytska, Colleen E. Larmour, Pichai Raman, Daniel Martinez, Gwenda F. Ligon, Jay S. Lillquist, Ulisse Cucchi, Paolo Orsini, Simona Rizzi, Bruce R. Pawel, Diego Alvarado and Yael P. Mossé

Sci Transl Med **11**, eaau9732.
DOI: 10.1126/scitranslmed.aau9732

No neuroblastomas left behind

Anaplastic lymphoma kinase (ALK) is frequently expressed in neuroblastoma, one of the more common pediatric cancers. Although small-molecule inhibitors of ALK are already in clinical use, the target protein often develops mutations that impede the effectiveness of these drugs. As an alternative to chemical inhibitors, Sano *et al* . developed an antibody-drug conjugate consisting of an antibody that recognizes ALK and a toxin that kills the ALK-expressing cells. The authors confirmed that ALK is not expressed in normal healthy tissues, indicating that this approach should be safe, and demonstrated the efficacy of the antibody-drug conjugate in mouse models of neuroblastoma with wild-type and mutant ALK.